



1     **Assessing Climate Change Impacts on Live Fuel Moisture and Wildfire Risk**  
2                                     **Using a Hydrodynamic Vegetation Model**

3     Wu Ma<sup>1</sup>, Lu Zhai<sup>2</sup>, Alexandria Pivovarov<sup>3</sup>, Jacquelyn Shuman<sup>4</sup>, Polly Buotte<sup>5</sup>, Junyan Ding<sup>6</sup>, Bradley  
4             Christoffersen<sup>7</sup>, Max Moritz<sup>8</sup>, Charles D. Koven<sup>6</sup>, Lara Kueppers<sup>9</sup>, Chonggang Xu<sup>1,\*</sup>

5     <sup>1</sup>*Earth and Environmental Sciences Division, Los Alamos National Laboratory, Los Alamos,*  
6     *NM, United States*

7     <sup>2</sup>*Department of Natural Ecology Resource and Management, Oklahoma State University,*  
8     *Stillwater, OK, United States*

9     <sup>3</sup>*Atmospheric Science and Global Change Division, Pacific Northwest National Laboratory,*  
10    *Richland, WA, United States*

11    <sup>4</sup>*National Center for Atmospheric Research, Climate and Global Dynamics, Terrestrial Sciences*  
12    *Section, Boulder, CO, United States*

13    <sup>5</sup>*Energy and Resources Group, University of California, Berkeley, CA, United States*

14    <sup>6</sup>*Climate and Ecosystem Sciences Division, Lawrence Berkeley National Laboratory, CA, United*  
15    *States*

16    <sup>7</sup>*Department of Biology, University of Texas Rio Grande Valley, Edinburg, TX, United States*

17    <sup>8</sup>*UC ANR Cooperative Extension, Bren School of Environmental Science & Management,*  
18    *University of California, Santa Barbara, CA, United States*

19    <sup>9</sup>*Energy and Resources Group, University of California, Berkeley, and Lawrence Berkeley*  
20    *National Laboratory, Berkeley, CA, United States*

21    \* *Corresponding author (Chonggang Xu, cxu@lanl.gov)*

22



23 **Abstract:** Live fuel moisture content (LFMC) plays a critical role in wildfire dynamics, but little  
24 is known about responses of LFMC to multivariate climate change, e.g., warming temperature,  
25 CO<sub>2</sub> fertilization and altered precipitation patterns, leading to a limited prediction ability of  
26 future wildfire risks. Here, we use a hydrodynamic vegetation model to estimate LFMC  
27 dynamics of chaparral shrubs, a dominant vegetation type in fire-prone southern California. We  
28 parameterize the model based on observed shrub allometry and hydraulic traits, and evaluate the  
29 model's accuracy through comparisons between simulated and observed LFMC of three plant  
30 functional types (PFTs) under current climate conditions. Moreover, we estimate the number of  
31 days per year of LFMC below 79% (which is a critical threshold for wildfire danger rating) from  
32 1950 to 2099 for each PFT, and compare the number of days below the threshold for medium  
33 and high greenhouse gas emission scenarios (RCP4.5 and 8.5). We find that climate change  
34 could lead to more days per year (5.5-15.2% increase) with LFMC below 79% from historical  
35 period 1950-1999 to future period 2075-2099, and therefore cause an increase in wildfire danger  
36 for chaparral shrubs in southern California. Under the high greenhouse gas emission scenario  
37 during the dry season, we find that the future LFMC reductions mainly result from a warming  
38 temperature, which leads to 9.5-19.1% reduction in LFMC. Lower precipitation in the spring  
39 leads to a 6.6-8.3% reduction in LFMC. The combined impacts of warming and precipitation  
40 change on fire season length are equal to the additive impacts of warming and precipitation  
41 change individually. Our results show that the CO<sub>2</sub> fertilization will mitigate fire risk by causing  
42 a 3.7-5.1% increase in LFMC. Our results suggest that multivariate climate change could cause a  
43 significant net reduction in LFMC and thus exacerbate future wildfire danger in chaparral shrub  
44 systems.



45 **Keywords:** FATES-HYDRO, chaparral shrubs, plant functional types, southern California, CO<sub>2</sub>  
46 enrichment, climate change

## 47 **1. Introduction**

48 Historical warming and changes in precipitation have already impacted wildfire at a  
49 global scale (e.g. Stocks et al. 1998; Gillett et al. 2004; Westerling et al. 2003, 2006) and it is  
50 expected that accelerating future warming will continue to significantly influence global wildfire  
51 regimes (e.g. Flannigan et al. 2009; Liu et al. 2010; Moritz et al. 2012). So far, prior studies have  
52 mainly focused on impacts of dead fuel moisture and weather conditions on wildfire. For  
53 example, dead fuel moisture is found to be related to fire ignition and fire spread potential (or  
54 potential area burnt) (Aguado et al. 2007; Caccamo et al. 2012a), and specific weather conditions  
55 such as increased vapor pressure deficit (Williams et al. 2019) can lead to a vast increase in fire  
56 activity (Goss et al. 2020). While previous studies provide great insights into fire risks with  
57 changes in climate and dead fuel moisture, there is still limited understanding of how climate  
58 change influences live fuel moisture content (LFMC) and the consequent wildfire risks. This is  
59 particularly true for the combined impacts of warming temperature, altered precipitation, and  
60 increasing CO<sub>2</sub> fertilization (Chuvieco et al. 2004; Pellizzaro 2007; Caccamo et al. 2012b;  
61 Williams et al. 2019; Goss et al. 2020).

62 A measure of water content within living leaves and fine branches in relation to their dry  
63 weight, LFMC has been found to be one of the most critical factors influencing combustion, fire  
64 spread, and fire consumption (e.g. Agee et al. 2002; Zarco-Tejada et al. 2003; Bilgili & Saglam  
65 2003; Yebra et al. 2008; Dennison et al. 2008; Anderson & Anderson 2010; Keeley et al. 2011).  
66 This is because a low fuel moisture content leads to increased flammability and a higher  
67 likelihood of ignition (Dimitrakopoulos & Papaioannou 2001). For instance, LFMC was found to



68 be a significant factor contributing to the occurrence of wildfires in Australia (Plucinski 2003),  
69 Spain (Chuvienco et al. 2009) and California (Santa Monica Mountains; Dennison et al. 2008;  
70 Dennison & Moritz 2009; Pivovaroff et al. 2019). Dennison & Moritz (2009) found strong  
71 evidence of a LFMC threshold, but near 79%, which may determine when large fires can occur.

72       Vegetation moisture content is dependent on both ecophysiological characteristics of the  
73 species and environmental conditions, including both climatic variables and soil water  
74 availability (Rothermel 1972; Castro et al. 2003; Castro et al. 2003; Pellizzaro 2007; Pivovaroff  
75 et al. 2019; Nolan et al. 2020). So far, little is known about the relative importance of different  
76 climate variables to future LFMC. On the one hand, warming could contribute to a higher  
77 atmospheric demand and higher evapotranspiration (Rind et al. 1990) and thus lead to a lower  
78 LFMC. On the other hand, higher CO<sub>2</sub> concentration will decrease stomatal conductance  
79 (Wullschleger et al. 2002) and plant water loss, and thus lead to a higher LFMC. The impacts of  
80 CO<sub>2</sub> and warming could be complicated by local changes in precipitation patterns and humidity  
81 (Mikkelsen et al. 2008).

82       The sensitivity of LFMC to climate change is likely to be affected by plant hydraulic  
83 traits (PFT, the plant properties that regulate water transport and storage within plant tissues),  
84 which affect plant water regulation (Wu et al. 2020). Hydraulic traits determine contrasting plant  
85 drought adaptation strategies when responding to dry conditions: 1) water stress avoiders and 2)  
86 water stress tolerators (Tobin et al. 1999; Wei et al. 2019). The “avoiders” generally have a more  
87 conservative hydraulic strategy under water stress by either closing stomata early, dropping  
88 leaves or accessing deep water to avoid more negative water potentials and therefore xylem  
89 cavitation. Meanwhile, the “tolerators” generally have a more aggressive hydraulic strategy by  
90 building xylem and leaves that are more resistant to cavitation so that they can tolerate more



91 negative water potential and continue to conduct photosynthesis under water stress. Therefore,  
92 compared with the tolerators, the avoiders normally have a lower sapwood density and higher  
93 plant water storage capacity in their tissues to avoid cavitation (Meinzer et al. 2003, 2009;  
94 Pineda-Garcia et al. 2013). Because the avoiders rely on water storage capacity as one way to  
95 avoid cavitation thereby maintaining a relatively high LFMC, and water loss from storage should  
96 increase with warming, LFMC should be more sensitive to climate change in avoiders relative to  
97 tolerators.

98         While over half of terrestrial landscapes on Earth are considered fire-prone (Krawchuk et  
99 al. 2009), Mediterranean-type climate regions are routinely impacted by fire, often on an annual  
100 basis. This is partly because Mediterranean climate regions are characterized by winter rains  
101 followed by annual summer drought, when no rainfall occurs for several months. Multiday  
102 periods of extreme temperatures, as well as katabatic hot, dry, and intense winds, often punctuate  
103 the annual drought, leading to some of the worst fire weather in the world (Schroeder et al.  
104 1964). This can result in wildfires that are large, high-intensity, and stand-replacing (Keeley  
105 1995; Keeley & Zedler 2009; Balch et al. 2017). Globally, Mediterranean climate regions are  
106 characterized by evergreen sclerophyllous-leaved shrublands. The Mediterranean climate region  
107 in California is dominated by chaparral, which is adapted to the periodic fire regime in California  
108 (Venturas et al. 2016). Previous studies have proposed a variety of relationships between  
109 chaparral LFMC and fire danger in southern California (Dennison et al. 2008; Dennison &  
110 Moritz 2009), but less is known about how climate changes could alter LFMC and fire danger. In  
111 chaparral, LFMC is usually high during the winter and spring (wet season) and then gradually  
112 declines during the dry season (summer and fall), which leads to a typical fire season  
113 approximately six months long in southern California (Pivovarov et al. 2019). One key risk is



114 that severe drought conditions are becoming exacerbated under climate change, which might  
115 lead to the occurrence of larger and higher-intensity fires in chaparral (Dennison et al. 2008;  
116 Dennison & Moritz 2009).

117         There has been a long history of wildfire modeling, with three types of models: 1) fine-  
118 scale fire behavior models (e.g. FIRETEC by Linn et al. 2002); 2) landscape-scale fire  
119 disturbance models (e.g. LANDIS-II by Sturtevant et al. 2009); and 3) global-scale fire dynamics  
120 models (e.g. SPITFIRE by Thonicke et al. 2010). While these models focus on simulation at  
121 different scales, their fire danger indices are mainly calculated from climate and dead fuel  
122 moisture and currently lack dynamic prediction of LFMC. One key limitation is that most  
123 previous models have not yet considered plant hydrodynamics (Holm et al. 2012; Xu et al. 2013;  
124 Seiler et al. 2014), which is integral to LFMC prediction. Recently, there have been important  
125 improvements to global dynamic vegetation models by incorporating plant hydrodynamics  
126 (Fisher et al. 2018). These models have been used to study the interaction between elevated CO<sub>2</sub>  
127 and drought (Duursma & Medlyn, 2012), the impact of hydraulic traits on plant drought response  
128 (Christofferson et al. 2016), the role of hydraulic diversity in vegetation response to drought (Xu  
129 et al. 2016) and hydroclimate change (Powell et al. 2018), and vegetation water stress and root  
130 water uptake (Kennedy et al. 2019). While the main purpose of the new hydraulic components is  
131 to improve the vegetation response to drought, the fact that hydrodynamic models consider tissue  
132 water content as a prognostic variable provides an opportunity to assess the climate impacts on  
133 LFMC.

134         The objective of this study is to quantify LFMC dynamics and associated changes in fire  
135 season duration for a chaparral ecosystem in southern California under climate change using a  
136 vegetation demographic model that incorporates plant hydraulics. We test one overarching



137 hypothesis: future climate change will decrease LFMC and result in a longer fire season as  
138 determined by a critical threshold of LFMC ( $H_0$ ). Specifically, we test the following four sub-  
139 hypotheses: 1) warming has a stronger impact on LFMC than  $\text{CO}_2$  fertilization ( $H_1$ ); 2) seasonal  
140 changes in precipitation lead to a longer fire season as determined by LFMC ( $H_2$ ); 3) the  
141 combined impacts of warming and precipitation on fire season length are equal to the additive  
142 impacts of warming and precipitation change individually ( $H_3$ ); and 4) plants with more  
143 conservative hydraulic strategies (“avoiders”) will be more sensitive to warming because their  
144 higher water storage capacity could be more vulnerable to warming ( $H_4$ ).

## 145 **2. Materials and Methods**

146 To understand climate change impacts on LFMC for the chaparral ecosystem, we applied  
147 the Functionally Assembled Terrestrial Simulator (FATES; Fisher et al. 2015; Massoud et al.  
148 2019; Koven et al. 2020) coupled with a hydrodynamic vegetation module (FATES-HYDRO;  
149 Christoffersen et al. 2016) in the Santa Monica Mountains in California. We validated the model  
150 using the observed LFMC for three chaparral shrub PFTs. Then, we applied FATES-HYDRO to  
151 estimate long-term dynamics of LFMC during 1950-2099 for each PFT using downscaled Earth  
152 System Model (ESM) climate scenarios. Based on the simulated LFMC, we evaluated wildfire  
153 danger based on the number of days per year of LFMC below the critical value of 79% from  
154 1950 to 2099 for each PFT under RCP 4.5 and 8.5. Finally, we assessed the relative importance  
155 of changes in individual and combined climate variables including  $\text{CO}_2$ , temperature,  
156 precipitation, and relative humidity and tested the corresponding hypotheses.

### 157 **2.1 Study site**



158 The study site is located at the Stunt Ranch Santa Monica Mountains Reserve, in the  
159 Santa Monica Mountains in California, USA (N 34° 05', W 118° 39'). Stunt Ranch is dominated  
160 by chaparral vegetation, with an elevation of approximately 350 m and a Mediterranean-type  
161 climate. The average maximum temperature is 31.5 °C and the average minimum temperature is  
162 4.6 °C. Mean annual precipitation is 478 mm, occurring mostly during the wet season (i.e.  
163 November-March) with almost no rainfall during the dry season (i.e. April-October). Soil texture  
164 information for Stunt Ranch is based on a national soil survey database  
165 (<https://websoilsurvey.sc.egov.usda.gov/App/WebSoilSurvey.aspx>; Table S1). We focused on  
166 PFTs representing 11 study species, including chamise (*Adenostoma fasciculatum* - Af), red  
167 shank (*Adenostoma sparsifolium* - As), big berry manzanita (*Arctostaphylos glauca* - Ag), buck  
168 brush (*Ceanothus cuneatus* - Cc), greenbark ceanothus (*Ceanothus spinosus* - Cs), mountain  
169 mahogany (*Cercocarpus betuloides* - Cb), toyon (*Heteromeles arbutifolia* - Ha), laurel sumac  
170 (*Malosma laurina* - Ml), scrub oak (*Quercus berberidifolia* - Qb), hollyleaf redberry (*Rhamnus*  
171 *ilicifolia* - Ri), and sugar bush (*Rhus ovata* - Ro). Detailed information about the study site and  
172 species characterizations found at Stunt Ranch can be found in Venturas et al. (2016) and  
173 Pivovarov et al. (2019).

## 174 **2.2 FATES-HYDRO model**

175 FATES is a vegetation demographic model (Fisher et al. 2015), which uses a size-  
176 structured group of plants (cohorts) and successional trajectory-based patches using the  
177 ecosystem demography approach (Moorcroft et al. 2001; Massoud et al. 2019). FATES simulates  
178 growth in part by integrating photosynthesis across different leaf layers for each cohort. FATES  
179 allocates photosynthetic carbon to storage and leaf, root, and stem tissues based on the allometry  
180 of different plant species (Koven et al. 2020). Mortality within FATES is mainly simulated by



181 carbon starvation caused by depletion of carbon storage and hydraulic function failure caused by  
182 embolism via the hydrodynamic model (Christoffersen et al. 2016). FATES is coupled with the  
183 Exascale Energy Earth System Model (E3SM, Caldwell et al., 2019) land model (ELM).

184 A key component of FATES, the plant hydrodynamic model (HYDRO; Christoffersen et  
185 al. 2016), simulates the water flow from soil through root, stem and leaf to the atmosphere. In  
186 this model, water flow is calculated based on water pressure gradients across different plant  
187 compartments (leaf, stem, transporting roots, absorbing roots and rhizosphere). Specifically, flow  
188 between compartment  $i$  and  $i + 1$  ( $Q_i$ ) is given by

$$Q_i = -K_i \Delta h_i \quad (1)$$

189 where  $K_i$  is the total conductance ( $\text{kg MPa}^{-1} \text{s}^{-1}$ ) at the boundary of compartments  $i$  and  $i + 1$  and  
190  $\Delta h_i$  is the total water potential difference between the compartments:

$$\Delta h_i = \rho_w g (z_i - z_{i+1}) + (\psi_i - \psi_{i+1}) \quad (2)$$

191 where  $z_i$  is compartment distance above (+) or below (-) the soil surface (m),  $\rho_w$  is the density of  
192 water ( $10^3 \text{ kg m}^{-3}$ ),  $g$  is acceleration due to gravity ( $9.8 \text{ m s}^{-2}$ ), and  $\psi_i$  is tissue or soil matric  
193 water potential (MPa).  $K_i$  is treated here as the product of a maximum boundary conductance  
194 between compartments  $i$  and  $i + 1$  ( $K_{max,i}$ ), and the fractional maximum hydraulic conductance  
195 of the adjacent compartments ( $FMC_i$  or  $FMC_{i+1}$ ), which is a function of the tissue water content.  
196 A key parameter that controls  $FMC$  is the critical water potential ( $P_{50}$ ) that leads to 50% loss of  
197 hydraulic conductivity. The tissue water potential is calculated based on pressure-volume (PV)  
198 theory (Tyree & Hammel, 1972; Tyree & Yang, 1990; Bartlett et al., 2012). For leaves, it is  
199 described by three phases: 1) capillary water phase with full turgor, 2) elastic drainage phase  
200 before reaching turgor loss point; and 3) post-turgor loss phase. For other tissues, it only has  
201 phases 2 and 3. Compared to a non-hydrodynamic model, this formulation allows the simulation



202 of plant water transport limitation on transpiration. For the non-hydrodynamic version of  
203 FATES, the water limitation factor for transpiration ( $B_{tran}$ ) is calculated based on the soil  
204 moisture potential (Fisher et al. 2015). For the hydrodynamic version,  $B_{tran}$  is calculated based on  
205 the leaf water potential ( $\psi_l$ ) (Christoffersen et al. 2016) as follows,

$$206 \quad B_{tran} = [1 + (\frac{\psi_l}{P_{50\_gs}})^{a_l}]^{-1}, \quad (3)$$

207 where  $P_{50\_gs}$  is the leaf water potential that leads to 50% loss of stomatal conductance and  $a_l$  is  
208 the shape parameter. Please refer to Christoffersen, et al. 2016 for details of formulations of  
209 *FMC* for different plant tissues.

210 Because the main purpose here is to assess L<sub>FMC</sub>, we controlled for variation in size  
211 structure that could arise from hydrodynamic trait or climate differences between model runs by  
212 using a reduced-complexity configuration of the model where growth and mortality are turned  
213 off and ecosystem structure is held constant. The plant sizes and number density are set based on  
214 a vegetation inventory from Venturas et al. (2016).

### 215 **2.3 Allometry and trait data for model parameterization**

216 FATES-HYDRO has a large number of parameters (>80; see Massoud et al. 2019 for a  
217 complete list except for hydraulic parameters). Based on a previous sensitivity analysis study  
218 (Massoud et al. 2019), we focused on estimating the most influential parameters for allometry,  
219 leaf and wood traits, and hydraulic traits from observations of 11 chaparral shrub species (see  
220 Supplementary, Table S2), collected from Jacobsen et al. (2008) and Venturas et al. (2016).  
221 Based on a hierarchical cluster analysis of allometry and trait data, the chaparral shrub species  
222 were classified into three PFTs (Fig. 1 and Table S3): a low productivity, aggressive hydraulic  
223 strategy PFT (PFT\_LPAH) with a relative low  $V_{c,max25}$  (the maximum carboxylation rate at 25



224 °C) and a very negative  $P_{50}$  (the leaf water potential leading to 50% loss of hydraulic  
225 conductivity); a medium productivity, conservative hydraulic strategy PFT (PFT\_MPCH)  
226 represented by a medium  $V_{c,max25}$  and a less negative  $P_{50}$ , turgor loss point and water potential at  
227 full turgor; and a high productivity, aggressive hydraulic strategy PFT (PFT\_HPAH) with a  
228 relatively high  $V_{c,max25}$  and a very negative  $P_{50}$ . The mean of species-level trait data weighted by  
229 species abundance at the site were used to parameterize FATES-HYDRO.

#### 230 **2.4 Live Fuel Moisture Content for model evaluation**

231 In this study, we used measured LFMC to validate the FATES-HYDRO predictions.  
232 LFMC (%) is the ratio of water weight to dry weight of living plant tissue (Burgan 1979). LFMC  
233 was measured approximately every three weeks, concurrently with plant water potentials in 2015  
234 and 2016 (Pivovarov et al. 2019). For comparison with our model outputs, we calculated the  
235 mean LFMC within leaves for each PFT weighted by the species abundance (Venturas et al.  
236 2016).

#### 237 **2.5 Climate drivers**

238 We forced the FATES-HYDRO model with temperature, relative humidity, precipitation,  
239 downward solar radiation, wind components, and specific humidity. Historical climate data  
240 during 2012-2019, which were used for FATES-HYDRO calibration, were extracted from a local  
241 weather station (<https://stuntranch.ucnrs.org/weather-date/>). Historical and future climate data  
242 during 1950-2099, which were used for simulations of LFMC by FATES-HYDRO model, were  
243 downloaded from the Multivariate Adaptive Constructed Analogs (MACA) datasets (Abatzoglou  
244 & Brown 2011; <http://maca.northwestknowledge.net>). The MACA datasets (1/24-degree or  
245 approximately 4-km; Abatzoglou & Brown 2011) include 20 ESMs with historical forcings



246 during 1950-2005 and future Representative Concentration Pathways (RCPs) RCP 4.5 and  
247 RCP8.5 scenarios during 2006-2099 from the native resolution of the ESMs. As training data for  
248 MACAv1/v2-METDATA, the gridded surface meteorological dataset METDATA (Abatzoglou,  
249 2013) were used with high spatial resolution (1/24-degree) and daily timescales for near-surface  
250 minimum/maximum temperature, minimum/maximum relative humidity, precipitation,  
251 downward solar radiation, wind components, and specific humidity.

## 252 **2.6 Hypothesis testing**

253 To test  $H_0$ , we compared the simulated LFMC under the climate projections from 20  
254 ESMs under RCP 4.5 and 8.5. We then tested if the LFMC during the April-October dry season  
255 in the historic period of 1950-1999 is significantly higher than that in the future period of 2075-  
256 2099. For the fire season duration, we estimated the number of days per year below a critical  
257 threshold of LFMC (79%). Similarly, we tested if the number of days per year below the critical  
258 threshold of LFMC during the historical period are significantly different from that during the  
259 future period.

260 To test  $H_1$ , we compared model outputs of mean LFMC and fire season length for three  
261 PFTs with/without  $CO_2$  changes (fixed  $CO_2$  at 367 ppm vs dynamic  $CO_2$  concentrations from  
262 RCP 4.5 or RCP 8.5) and warming. To remove the future warming trend, future temperature was  
263 replaced with historical (1986-2005) temperature data for every 20 year period. Similarly, to test  
264  $H_2$ , we compared the model outputs of LFMC and fire season length for three PFTs with/without  
265 precipitation changes. To test  $H_3$ , we compared model outputs of LFMC and fire season length  
266 for three PFTs under three scenarios: 1) without warming; 2) without precipitation changes; and  
267 3) without warming and precipitation changes. Finally, to test  $H_4$ , we compared model outputs of  
268 LFMC and fire season length across the three different PFTs with different hydraulic strategies.



## 269 **3. Results**

### 270 **3.1 Comparison between simulated and measured LFMC**

271 Our results showed that FATES-HYDRO was able to capture variation in the LFMC for  
272 different PFTs (Fig. 2). Specifically, the model was able to capture 93%, 88%, and 82% of the  
273 variance in observed LFMC for the period of 2015-2016 for three PFTs, respectively (Fig. 2 b, d,  
274 f). The model was also able to capture the seasonal dynamics of LFMC in comparison to  
275 observed data (Fig. 2 a, c, e).

### 276 **3.2 Changes in the LFMC and fire season length from historical to future periods**

277 Using the validated model driven by climate projections from 20 ESMs under greenhouse  
278 gas emission scenarios RCP4.5 and RCP 8.5, we found that the daily mean LFMC during the  
279 future period of 2075-2099 was projected to become significantly lower than that during the  
280 historical period of 1950-1999 for all three PFTs (Fig 3,  $P < 0.0001$ ). Specifically, the histogram  
281 of daily mean LFMC during the April-October dry season showed that there was a higher  
282 probability of low LFMC under future climate conditions (Fig. S1). The daily mean LFMC  
283 decreased from 84.9%, 101.5%, and 78.6% during the historical period of 1950-1999 to 81.3-  
284 83.1%, 96.6-99.2%, and 75.1-76.9% during the future period of 2075-2099 under both climate  
285 scenarios for PFT\_LPAH, PFT\_MPCH, PFT\_HPAH, respectively (Fig 3).

286 Based on the projected LFMC, there was a significant increase in the fire season length  
287 with the critical threshold of LFMC from the historical period of 1950-1999 to the future period  
288 of 2075-2099 for three PFTs. With the critical threshold of 79% LFMC, the fire season length  
289 was projected to increase by 21, 23, 20 days under RCP 8.5 (Fig. 4 and Table S4), and to  
290 increase by 10, 12, 9 days under RCP 4.5 (Fig. 4 and Table S4). The above results for mean



291 LFMC and fire season length support hypothesis H<sub>0</sub> that future climate change will decrease  
292 LFMC and result in a longer fire season, as determined by critical thresholds for LFMC, for all  
293 three PFTs.

### 294 **3.3 Relative effects of individual climate changes on the length of the fire season**

295 In order to better understand the relative contribution to fire season length of different  
296 climate variables, we ran FATES-HYDRO for three PFTs using meteorological forcings that  
297 isolated and removed changes in individual specific variables. Our results showed that the  
298 increase in fire season length mainly resulted from warming, which led to 17-24 days (9.5-  
299 19.1%) per year increase in fire season length for the critical threshold of 79% LFMC under RCP  
300 8.5 (Fig. 5). For RCP 4.5, the warming contributed to 6-7 days (4.1-4.7%) per year increase in  
301 fire season length (Fig. 5). We also found that elevated CO<sub>2</sub> concentrations decreased fire season  
302 length with 7-8 days (3.7-5.1%) per year decrease in fire season length under RCP 8.5 (Fig. 5).  
303 Under RCP 4.5, CO<sub>2</sub> increases led to 2-3 days (1.7-2.4%) per year decrease in fire season length  
304 (Fig. 5). Because the impact of warming on fire season length was stronger than the mitigation  
305 from CO<sub>2</sub> enrichment, our results support hypothesis H<sub>1</sub>.

306 Even though total precipitation was projected to increase in the future, lower precipitation  
307 in the spring and autumn (Fig. S2 a, b) led to 9-11 days (6.6-8.3%) per year increase in fire  
308 season length with the critical threshold of 79% LFMC under RCP 8.5 (Fig. 5). Under RCP 4.5,  
309 the precipitation changes contributed to 1-3 days (0.9-1.7%) increase in fire season length (Fig.  
310 5). This result supported hypothesis H<sub>2</sub> that seasonal changes in precipitation lead to a longer fire  
311 season as determined by LFMC.



312 Our results showed that the combined impacts of warming and precipitation on fire  
313 season length were equal to the additive impacts of warming and precipitation change  
314 individually. This supported hypothesis H<sub>3</sub>. Specifically, the combined changes in temperature  
315 and precipitation caused 26-35 days per year (16.1-27.4%) increase in fire season length with the  
316 critical threshold of 79% LFMC under RCP 8.5 (Fig. 5). Under RCP 4.5, the combined changes  
317 in temperature and precipitation caused a 7-10 days per year (5.0-6.4%) change in fire season  
318 length.

### 319 **3.4 Comparison of changes in fire season length among three PFTs under climate change**

320 Regarding three PFTs under both climate scenarios, fire season length of PFT\_HPAH  
321 was the longest (165-176 days per year), while fire season length of PFT\_MPCH was the  
322 shortest (113-124 per year) during 2075-2099 (Fig. 4). However, the response of fire season  
323 length to warming was strongest for PFT\_MPCH. Specifically, for PFT\_MPCH, warming under  
324 RCP 8.5 led to an increase of 23 days in fire season length (Fig. 5 b) and warming under RCP  
325 4.5 led to an increase of 12 days in fire season length. For PFT\_LPAH, warming under RCP 8.5  
326 led to an increase of 21 days in fire season length (Fig. 5 a) while warming under RCP 4.5 led to  
327 an increase of 10 days in fire season length. Finally, for PFT\_HPAH, warming under RCP 8.5  
328 led to an increase of 19 days in fire season length (Fig. 5 c) and 9 days in fire season length with  
329 under RCP 4.5. Because PFT\_MPCH has a more conservative hydraulic strategy with less  
330 negative P<sub>50</sub>, turgor loss point and water potential at full turgor, this result supported hypothesis  
331 H<sub>4</sub> that the more conservative hydraulic strategy will be more sensitive to warming.

## 332 **4. Discussion**



333           Low LFMC within shrub leaves and small branches increases the flammability and  
334 likelihood of combustion, making it vitally important to monitor temporal variations in LFMC,  
335 especially during the dry season (Dennison et al, 2008). The strong relationships between  
336 observed and simulated LFMC of all PFTs suggested that the plant hydrodynamic model,  
337 FATES-HYDRO, could accurately estimate LFMC seasonal dynamics, and consequently be  
338 useful to predict fire risks in Mediterranean-type climate regions. During the future period (2075-  
339 2099) and the historical period (1950-1999), both periods displayed lower values in the dry  
340 season (April - October), which is consistent with lower LFMC during the summer-fall dry  
341 season, rather than the winter-spring wet season (Chuvieco et al, 2004; Pellizzaro et al, 2007;  
342 Pivovarovoff et al. 2019). Extremely low daily LFMC was more likely to occur during the future  
343 period, which had higher temperature than the historical period. From the historical to the future  
344 period, fire season length could increase by 5.5-15.2% as determined by the critical threshold of  
345 LFMC of 79% under climate change for chaparral shrub ecosystems ( $H_0$ ).

346 Quantifying influences of climatic variables on LFMC is crucial to predicting future fire risks  
347 (Dennison & Moritz, 2009). Our results showed that future warming was the most important  
348 driver of LFMC. This finding suggested that higher temperature would substantially decrease  
349 LFMC and strongly increase the fire season length, which may greatly increase fire risks in the  
350 future (e.g. Dennison et al, 2008; Chuvieco et al, 2009; Pimont et al, 2019). CO<sub>2</sub> fertilization is  
351 expected to reduce stomatal conductance (Pataki et al. 2000; Tognetti et al. 2000) and thus could  
352 mitigate the impacts of warming on LFMC. Our results displayed that, even though the CO<sub>2</sub>  
353 impact did cause a 3.7-5.1% reduction in fire season length, the impact of warming on fire  
354 season length is about 5.8-14% larger than the CO<sub>2</sub> effect ( $H_1$ ). This result suggests that CO<sub>2</sub>  
355 fertilization cannot offset the LFMC impacts from warming. The FATES-HYDRO model



356 assumes a consistent stomatal sensitivity to CO<sub>2</sub> concentration across Mediterranean shrub  
357 species. While Mediterranean shrub species in arid and semi-arid systems would vary in their  
358 stomatal response in the real world (Pataki et al. 2000). Therefore, our model may overestimate  
359 the CO<sub>2</sub> effect on stomatal conductance and its mitigating influence might be smaller in reality  
360 for some species.

361 Previous studies implied that the timing of precipitation may have a strong impact on  
362 subsequent LFMC (e.g. Veblen et al. 2000; Westerling et al. 2006; Dennison & Moritz 2009). In  
363 this study, precipitation was also the key driver of LFMC under future climate conditions. Our  
364 results showed that, even though total precipitation was projected to increase, the reduction in  
365 spring and autumn precipitation was projected to cause a longer fire season length (H<sub>2</sub>; Fig. 5).  
366 This result was in agreement with a prior study indicating that spring precipitation, particularly  
367 in the month of March, was found to be the primary driver of timing of LFMC changes  
368 (Dennison & Moritz 2009). We also found that the combined impacts of warming and  
369 precipitation on fire season length were equal to the linearly additive impacts of warming and  
370 precipitation change individually (H<sub>3</sub>). Our results suggested that, when evaluating future fire  
371 risks, it is critical that we considered the seasonal changes in precipitation and its interaction with  
372 the warming impact.

373 Modeled vegetation responses to environmental changes could be determined by  
374 variations in traits (Koven et al, 2020). For three PFTs co-occurred in the simulations, even  
375 though they grew together and showed similar patterns in LFMC in response to climate change  
376 during 1950-2099, we did see some critical differences. Specifically, the plant functional type  
377 (PFT\_MPCH) with more conservative hydraulic strategy had the strongest responses to climate  
378 change (Fig. 5). This could be related to the fact that the PFT\_MPCH is more conservative in



379 terms of hydraulic strategy with less negative  $P_{50}$ , turgor loss point, and water potential at full  
380 turgor. The PFT\_MPCH plants had a relatively high saturated water content based on observed  
381 data (Fig 2) and the water within plant tissues could change more quickly in response to the  
382 environmental condition changes ( $H_4$ ).

### 383 **5. Conclusions**

384 A hydrodynamic vegetation model, FATES-HYDRO, was used to estimate historical and  
385 future LFMC dynamics of chaparral shrub species in southern California under climate change.  
386 FATES-HYDRO model was validated using monthly mean LFMC for three PFTs. The fire  
387 season length was projected to substantially increase under both climate scenarios from 1950-  
388 1999 to 2075-2099. This could increase wildlife risk over time for chaparral shrubs in southern  
389 California. Our results showed that temperature was the most important driver of LFMC and  
390 relative humidity was the least important among four climatic variables including  $CO_2$ ,  
391 temperature, precipitation, and relative humidity. The LFMC estimated by the FATES-HYDRO  
392 model offered a baseline of predicting plant hydraulic dynamics subjected to climate change and  
393 provided a critical foundation that reductions in LFMC from climate warming may exacerbate  
394 future wildfire risk.

### 395 **Acknowledgements**

396 This project is supported by the University of California Office of the President Lab Fees  
397 Research Program and the Next Generation Ecosystem Experiment (NGEE) Tropics, which is  
398 supported by the U.S. DOE Office of Science. CDK and JD are supported by the DOE Office of  
399 Science, Regional and Global Model Analysis Program, Early Career Research Program.

### 400 **References**



- 401 Abatzoglou JT (2013) Development of gridded surface meteorological data for ecological  
402 applications and modelling. *International Journal of Climatology*, 33, 121-131.
- 403 Agee, J.K., Wright, C.S., Williamson, N. and Huff, M.H., 2002. Foliar moisture content of  
404 Pacific Northwest vegetation and its relation to wildland fire behavior. *Forest ecology and*  
405 *management*, 167(1-3), pp.57-66.
- 406 Anderson, S.A. and Anderson, W.R., 2010. Ignition and fire spread thresholds in gorse (*Ulex*  
407 *europaeus*). *International Journal of Wildland Fire*, 19(5), pp.589-598.
- 408 Aguado, I., Chuvieco, E., Boren, R. and Nieto, H., 2007. Estimation of dead fuel moisture  
409 content from meteorological data in Mediterranean areas. Applications in fire danger assessment.  
410 *International Journal of Wildland Fire*, 16(4), pp.390-397.
- 411 Burgan, R.E. Estimating Live Fuel Moisture for the 1978 National Fire Danger Rating System;  
412 Intermountain Forest and Range Experiment Station: Ogden, UT, USA, 1979.
- 413 Bilgili, E. and Saglam, B., 2003. Fire behavior in maquis fuels in Turkey. *Forest Ecology and*  
414 *Management*, 184(1-3), pp.201-207.
- 415 Balch, J.K., Bradley, B.A., Abatzoglou, J.T., Nagy, R.C., Fusco, E.J. and Mahood, A.L., 2017.  
416 Human-started wildfires expand the fire niche across the United States. *Proceedings of the*  
417 *National Academy of Sciences*, 114(11), pp.2946-2951.
- 418 Bartlett, M.K., Scoffoni, C. and Sack, L., 2012. The determinants of leaf turgor loss point and  
419 prediction of drought tolerance of species and biomes: a global meta-analysis. *Ecology letters*,  
420 15(5), pp.393-405.



- 421 Christoffersen, B.O., Gloor, M., Fauset, S., Fyllas, N.M., Galbraith, D.R., Baker, T.R., Kruijt, B.,  
422 Rowland, L., Fisher, R.A., Binks, O.J. and Sevanto, S., 2016. Linking hydraulic traits to tropical  
423 forest function in a size-structured and trait-driven model (TFS v. 1-Hydro). *Geoscientific Model*  
424 *Development*, 9: 4227-4255.
- 425 Caccamo, G., Chisholm, L.A., Bradstock, R.A. and Puotinen, M.L., 2012a. Using remotely-  
426 sensed fuel connectivity patterns as a tool for fire danger monitoring. *Geophysical Research*  
427 *Letters*, 39(1).
- 428 Caccamo, G., Chisholm, L.A., Bradstock, R.A., Puotinen, M.L. and Phippen, B.G., 2012b.  
429 Monitoring live fuel moisture content of heathland, shrubland and sclerophyll forest in south-  
430 eastern Australia using MODIS data. *International Journal of Wildland Fire*, 21(3), pp.257-269.
- 431 Chuvieco, E., Cocero, D., Riano, D., Martin, P., Martínez-Vega, J., de la Riva, J. and Pérez, F.,  
432 2004. Combining NDVI and surface temperature for the estimation of live fuel moisture content  
433 in forest fire danger rating. *Remote Sensing of Environment*, 92(3), pp.322-331.
- 434 Caldwell, P.M., Mametjanov, A., Tang, Q., Van Roekel, L.P., Golaz, J.C., Lin, W., Bader, D.C.,  
435 Keen, N.D., Feng, Y., Jacob, R. and Maltrud, M.E., 2019. The DOE E3SM coupled model  
436 version 1: Description and results at high resolution. *Journal of Advances in Modeling Earth*  
437 *Systems*, 11(12), pp.4095-4146.
- 438 Castro, F.X., Tudela, A. and Sebastià, M.T., 2003. Modeling moisture content in shrubs to  
439 predict fire risk in Catalonia (Spain). *Agricultural and Forest Meteorology*, 116(1-2), pp.49-59.
- 440 Chuvieco, E., González, I., Verdú, F., Aguado, I. and Yebra, M., 2009. Prediction of fire  
441 occurrence from live fuel moisture content measurements in a Mediterranean ecosystem.  
442 *International Journal of Wildland Fire*, 18(4), pp.430-441.



- 443 Collins, M., Knutti, R., Arblaster, J., Dufresne, J.L., Fichefet, T., Friedlingstein, P., Gao, X.,  
444 Gutowski, W.J., Johns, T., Krinner, G. and Shongwe, M., 2013. Long-term climate change:  
445 projections, commitments and irreversibility. In *Climate Change 2013-The Physical Science*  
446 *Basis: Contribution of Working Group I to the Fifth Assessment Report of the Intergovernmental*  
447 *Panel on Climate Change* (pp. 1029-1136). Cambridge University Press.
- 448 Cook, B.I., Smerdon, J.E., Seager, R. and Coats, S., 2014. Global warming and 21 st century  
449 drying. *Climate Dynamics*, 43(9-10), pp.2607-2627.
- 450 Dennison, P.E., Moritz, M.A. and Taylor, R.S., 2008. Evaluating predictive models of critical  
451 live fuel moisture in the Santa Monica Mountains, California. *International Journal of Wildland*  
452 *Fire*, 17(1), pp.18-27.
- 453 Dennison, P.E. and Moritz, M.A., 2009. Critical live fuel moisture in chaparral ecosystems: a  
454 threshold for fire activity and its relationship to antecedent precipitation. *International Journal of*  
455 *Wildland Fire*, 18(8), pp.1021-1027.
- 456 Dimitrakopoulos, A.P. and Papaioannou, K.K., 2001. Flammability assessment of Mediterranean  
457 forest fuels. *Fire Technology*, 37(2), pp.143-152.
- 458 Dai, A., 2013. Increasing drought under global warming in observations and models. *Nature*  
459 *climate change*, 3(1), pp.52-58.
- 460 Duursma, R.A. and Medlyn, B.E., 2012. MAESPA: a model to study interactions between water  
461 limitation, environmental drivers and vegetation function at tree and stand levels, with an  
462 example application to [CO<sub>2</sub>] $\times$ drought interactions.



- 463 Flannigan, M.D., Krawchuk, M.A., de Groot, W.J., Wotton, B.M. and Gowman, L.M., 2009.  
464 Implications of changing climate for global wildland fire. *International journal of wildland fire*,  
465 18(5), pp.483-507.
- 466 Fisher, R.A., Williams, M., Da Costa, A.L., Malhi, Y., Da Costa, R.F., Almeida, S. and Meir, P.,  
467 2007. The response of an Eastern Amazonian rain forest to drought stress: results and modelling  
468 analyses from a throughfall exclusion experiment. *Global Change Biology*, 13(11), pp.2361-  
469 2378.
- 470 Fisher, R.A., Muszala, S., Versteinstein, M., Lawrence, P., Xu, C., McDowell, N.G., Knox, R.G.,  
471 Koven, C., Holm, J., Rogers, B.M. and Spessa, A., 2015. Taking off the training wheels: the  
472 properties of a dynamic vegetation model without climate envelopes, CLM4. 5 (ED).  
473 *Geoscientific Model Development*, 8(11), pp.3593-3619.
- 474 Fisher, R.A., Koven, C.D., Anderegg, W.R., Christoffersen, B.O., Dietze, M.C., Farrior, C.E.,  
475 Holm, J.A., Hurtt, G.C., Knox, R.G., Lawrence, P.J. and Lichstein, J.W., 2018. Vegetation  
476 demographics in Earth System Models: A review of progress and priorities. *Global change*  
477 *biology*, 24(1), pp.35-54.
- 478 Gillett, N.P., Weaver, A.J., Zwiers, F.W. and Flannigan, M.D., 2004. Detecting the effect of  
479 climate change on Canadian forest fires. *Geophysical Research Letters*, 31(18).
- 480 Goss, M., Swain, D.L., Abatzoglou, J.T., Sarhadi, A., Kolden, C.A., Williams, A.P. and  
481 Duffenbaugh, N.S., 2020. Climate change is increasing the likelihood of extreme autumn wildfire  
482 conditions across California. *Environmental Research Letters*, 15(9), p.094016.



- 483 Holm, J.A., Shugart, H.H., Van Bloem, S.J. and Larocque, G.R., 2012. Gap model development,  
484 validation, and application to succession of secondary subtropical dry forests of Puerto Rico.  
485 *Ecological Modelling*, 233, pp.70-82.
- 486 Jacobsen, A. L., Pratt, R. B., Davis, S. D., & Ewers, F. W. (2008). Comparative community  
487 physiology: nonconvergence in water relations among three semi-arid shrub communities. *New*  
488 *Phytologist*, 180(1), 100-113.
- 489 Konings, A.G., Rao, K. and Steele-Dunne, S.C., 2019. Macro to micro: microwave remote  
490 sensing of plant water content for physiology and ecology. *New Phytologist*, 223(3), pp.1166-  
491 1172.
- 492 Keeley, J.E., 1995. Future of California floristics and systematics: wildfire threats to the  
493 California flora. *Madrono*, pp.175-179.
- 494 Keeley, J.E. and Zedler, P.H., 2009. Large, high-intensity fire events in southern California  
495 shrublands: debunking the fine-grain age patch model. *Ecological Applications*, 19(1), pp.69-94.
- 496 Keeley, J.E., Bond, W.J., Bradstock, R.A., Pausas, J.G. and Rundel, P.W., 2011. *Fire in*  
497 *Mediterranean ecosystems: ecology, evolution and management*. Cambridge University Press.
- 498 Kennedy, D., Swenson, S., Oleson, K.W., Lawrence, D.M., Fisher, R., Lola da Costa, A.C. and  
499 Gentine, P., 2019. Implementing plant hydraulics in the community land model, version 5.  
500 *Journal of Advances in Modeling Earth Systems*, 11(2), pp.485-513.
- 501 Koven, C.D., Knox, R.G., Fisher, R.A., Chambers, J.Q., Christoffersen, B.O., Davies, S.J.,  
502 Detto, M., Dietze, M.C., Faybishenko, B., Holm, J. and Huang, M., 2020. Benchmarking and  
503 parameter sensitivity of physiological and vegetation dynamics using the Functionally



- 504 Assembled Terrestrial Ecosystem Simulator (FATES) at Barro Colorado Island, Panama.  
505 *Biogeosciences*, 17(11), pp.3017-3044.
- 506 Krawchuk, M.A., Moritz, M.A., Parisien, M.A., Van Dorn, J. and Hayhoe, K., 2009. Global  
507 pyrogeography: the current and future distribution of wildfire. *PloS one*, 4(4), p.e5102.
- 508 Linn, R., Reisner, J., Colman, J.J. and Winterkamp, J., 2002. Studying wildfire behavior using  
509 FIRETEC. *International journal of wildland fire*, 11(4), pp.233-246.
- 510 Liu, Y., Stanturf, J. and Goodrick, S., 2010. Trends in global wildfire potential in a changing  
511 climate. *Forest ecology and management*, 259(4), pp.685-697.
- 512 Massoud, E.C., Xu, C., Fisher, R.A., Knox, R.G., Walker, A.P., Serbin, S.P., Christoffersen,  
513 B.O., Holm, J.A., Kueppers, L.M., Ricciuto, D.M. and Wei, L., 2019. Identification of key  
514 parameters controlling demographically structured vegetation dynamics in a land surface model:  
515 CLM4. 5 (FATES). *Geoscientific Model Development*, 12(9), pp.4133-4164.
- 516 Moorcroft, P.R., Hurtt, G.C. and Pacala, S.W., 2001. A method for scaling vegetation dynamics:  
517 the ecosystem demography model (ED). *Ecological monographs*, 71(4), pp.557-586.
- 518 Mikkelsen, T.N., Beier, C., Jonasson, S., Holmstrup, M., Schmidt, I.K., Ambus, P., Pilegaard,  
519 K., Michelsen, A., Albert, K., Andresen, L.C. and Arndal, M.F., 2008. Experimental design of  
520 multifactor climate change experiments with elevated CO<sub>2</sub>, warming and drought: the  
521 CLIMAITE project. *Functional Ecology*, 22(1), pp.185-195.
- 522 Moritz, M.A., Parisien, M.A., Batllori, E., Krawchuk, M.A., Van Dorn, J., Ganz, D.J. and  
523 Hayhoe, K., 2012. Climate change and disruptions to global fire activity. *Ecosphere*, 3(6), pp.1-  
524 22.



- 525 Manabe, S. and Wetherald, R.T., 1975. The effects of doubling the CO<sub>2</sub> concentration on the  
526 climate of a general circulation model. *Journal of the Atmospheric Sciences*, 32(1), pp.3-15.
- 527 Meinzer, F.C., James, S.A., Goldstein, G. and Woodruff, D., 2003. Whole-tree water transport  
528 scales with sapwood capacitance in tropical forest canopy trees. *Plant, Cell & Environment*,  
529 26(7), pp.1147-1155.
- 530 Meinzer, F.C., Johnson, D.M., Lachenbruch, B., McCulloh, K.A. and Woodruff, D.R., 2009.  
531 Xylem hydraulic safety margins in woody plants: coordination of stomatal control of xylem  
532 tension with hydraulic capacitance. *Functional Ecology*, 23(5), pp.922-930.
- 533 Nolan, R.H., Blackman, C.J., de Dios, V.R., Choat, B., Medlyn, B.E., Li, X., Bradstock, R.A.  
534 and Boer, M.M., 2020. Linking forest flammability and plant vulnerability to drought. *Forests*,  
535 11(7), p.779.
- 536 Pivovarov, A. L., Emery, N., Sharifi, M. R., Witter, M., Keeley, J. E., & Rundel, P. W. (2019).  
537 The effect of ecophysiological traits on live fuel moisture content. *Fire*, 2(2), 28.
- 538 Powell, T.L., Koven, C.D., Johnson, D.J., Faybishenko, B., Fisher, R.A., Knox, R.G., McDowell,  
539 N.G., Condit, R., Hubbell, S.P., Wright, S.J. and Chambers, J.Q., 2018. Variation in  
540 hydroclimate sustains tropical forest biomass and promotes functional diversity. *New*  
541 *Phytologist*, 219(3), pp.932-946.
- 542 Pellizzaro, G., Cesaraccio, C., Duce, P., Ventura, A. and Zara, P., 2007. Relationships between  
543 seasonal patterns of live fuel moisture and meteorological drought indices for Mediterranean  
544 shrubland species. *International Journal of Wildland Fire*, 16(2), pp.232-241.



- 545 Plucinski, M.P., 2003. The investigation of factors governing ignition and development of fires  
546 in heathland vegetation. *PhD thesis. University of New South Wales, Sydney.*
- 547 Pimont, F., Ruffault, J., Martin-StPaul, N.K. and Dupuy, J.L., 2019. Why is the effect of live fuel  
548 moisture content on fire rate of spread underestimated in field experiments in shrublands?.  
549 *International journal of wildland fire*, 28(2), pp.127-137.
- 550 Pataki, D.E., Huxman, T.E., Jordan, D.N., Zitzer, S.F., Coleman, J.S., Smith, S.D., Nowak, R.S.  
551 and Seemann, J.R., 2000. Water use of two Mojave Desert shrubs under elevated CO<sub>2</sub>. *Global*  
552 *Change Biology*, 6(8), pp.889-897.
- 553 Pineda-Garcia, F., Paz, H. and Meinzer, F.C., 2013. Drought resistance in early and late  
554 secondary successional species from a tropical dry forest: the interplay between xylem resistance  
555 to embolism, sapwood water storage and leaf shedding. *Plant, Cell & Environment*, 36(2),  
556 pp.405-418.
- 557 Rind, D., Goldberg, R., Hansen, J., Rosenzweig, C. and Ruedy, R., 1990. Potential  
558 evapotranspiration and the likelihood of future drought. *Journal of Geophysical Research:*  
559 *Atmospheres*, 95(D7), pp.9983-10004.
- 560 Rothermel, R.C., 1972. *A mathematical model for predicting fire spread in wildland fuels* (Vol.  
561 115). Intermountain Forest & Range Experiment Station, Forest Service, US Department of  
562 Agriculture.
- 563 Sturtevant, B.R., Scheller, R.M., Miranda, B.R., Shinneman, D. and Syphard, A., 2009.  
564 Simulating dynamic and mixed-severity fire regimes: a process-based fire extension for  
565 LANDIS-II. *Ecological Modelling*, 220(23), pp.3380-3393.



- 566 Stocks, B.J., Fosberg, M.A., Lynham, T.J., Mearns, L., Wotton, B.M., Yang, Q., Jin, J.Z.,  
567 Lawrence, K., Hartley, G.R., Mason, J.A. and McKenney, D.W., 1998. Climate change and  
568 forest fire potential in Russian and Canadian boreal forests. *Climatic change*, 38(1), pp.1-13.
- 569 Schroeder, M.J., Glovinsky, M., Henricks, V.F., Hood, F.C. and Hull, M.K., 1964. *Synoptic*  
570 *weather types associated with critical fire weather*. USDA Forest Service, Pacific Southwest  
571 Range and Experiment Station. Berkeley, CA.
- 572 Seiler, C., Hutjes, R.W.A., Kruijt, B., Quispe, J., Añez, S., Arora, V.K., Melton, J.R., Hickler, T.  
573 and Kabat, P., 2014. Modeling forest dynamics along climate gradients in Bolivia. *Journal of*  
574 *Geophysical Research: Biogeosciences*, 119(5), pp.758-775.
- 575 Sheffield, J. and Wood, E.F., 2008. Projected changes in drought occurrence under future global  
576 warming from multi-model, multi-scenario, IPCC AR4 simulations. *Climate dynamics*, 31(1),  
577 pp.79-105.
- 578 Thonicke, K., Spessa, A., Prentice, I.C., Harrison, S.P., Dong, L. and Carmona-Moreno, C.,  
579 2010. The influence of vegetation, fire spread and fire behaviour on biomass burning and trace  
580 gas emissions: results from a process-based model. *Biogeosciences*, 7(6), pp.1991-2011.
- 581 Tyree, M.T. and Hammel, H.T., 1972. The measurement of the turgor pressure and the water  
582 relations of plants by the pressure-bomb technique. *Journal of experimental Botany*, 23(1),  
583 pp.267-282.
- 584 Tyree, M.T. and Yang, S., 1990. Water-storage capacity of Thuja, Tsuga and Acer stems  
585 measured by dehydration isotherms. *Planta*, 182(3), pp.420-426.



- 586 Tognetti, R., Minnocci, A., Peñuelas, J., Raschi, A. and Jones, M.B., 2000. Comparative field  
587 water relations of three Mediterranean shrub species co-occurring at a natural CO<sub>2</sub> vent. *Journal*  
588 *of Experimental Botany*, 51(347), pp.1135-1146.
- 589 Venturas, M. D., MacKinnon, E. D., Dario, H. L., Jacobsen, A. L., Pratt, R. B., & Davis, S. D.  
590 (2016). Chaparral shrub hydraulic traits, size, and life history types relate to species mortality  
591 during California's historic drought of 2014. *PLOS One*, 11(7).
- 592 Veblen, T.T., Kitzberger, T. and Donnegan, J., 2000. Climatic and human influences on fire  
593 regimes in ponderosa pine forests in the Colorado Front Range. *Ecological applications*, 10(4),  
594 pp.1178-1195.
- 595 Westerling, A.L., Gershunov, A., Brown, T.J., Cayan, D.R. and Dettinger, M.D., 2003. Climate  
596 and wildfire in the western United States. *Bulletin of the American Meteorological Society*,  
597 84(5), pp.595-604.
- 598 Westerling, A.L., Hidalgo, H.G., Cayan, D.R. and Swetnam, T.W., 2006. Warming and earlier  
599 spring increase western US forest wildfire activity. *science*, 313(5789), pp.940-943.
- 600 Williams, A.P., Abatzoglou, J.T., Gershunov, A., Guzman-Morales, J., Bishop, D.A., Balch, J.K.  
601 and Lettenmaier, D.P., 2019. Observed impacts of anthropogenic climate change on wildfire in  
602 California. *Earth's Future*, 7(8), pp.892-910.
- 603 Wullschlegel, S.D., Gunderson, C.A., Hanson, P.J., Wilson, K.B. and Norby, R.J., 2002.  
604 Sensitivity of stomatal and canopy conductance to elevated CO<sub>2</sub> concentration–interacting  
605 variables and perspectives of scale. *New Phytologist*, 153(3), pp.485-496.



- 606 Wu, J., Serbin, S.P., Ely, K.S., Wolfe, B.T., Dickman, L.T., Grossiord, C., Michaletz, S.T.,  
607 Collins, A.D., Detto, M., McDowell, N.G. and Wright, S.J., 2020. The response of stomatal  
608 conductance to seasonal drought in tropical forests. *Global Change Biology*, 26(2), pp.823-839.
- 609 Wei, L., Xu, C., Jansen, S., Zhou, H., Christoffersen, B.O., Pockman, W.T., Middleton, R.S.,  
610 Marshall, J.D. and McDowell, N.G., 2019. A heuristic classification of woody plants based on  
611 contrasting shade and drought strategies. *Tree physiology*, 39(5), pp.767-781.
- 612 Xu, C., McDowell, N.G., Sevanto, S. and Fisher, R.A., 2013. Our limited ability to predict  
613 vegetation dynamics under water stress. *New Phytologist*, 200(2), pp.298-300.
- 614 Xu, X., Medvigy, D., Powers, J.S., Becknell, J.M. and Guan, K., 2016. Diversity in plant  
615 hydraulic traits explains seasonal and inter-annual variations of vegetation dynamics in  
616 seasonally dry tropical forests. *New Phytologist*, 212(1), pp.80-95.
- 617 Yebra, M., Chuvieco, E. and Riaño, D., 2008. Estimation of live fuel moisture content from  
618 MODIS images for fire risk assessment. *Agricultural and forest meteorology*, 148(4), pp.523-  
619 536.
- 620 Yebra, M., Dennison, P.E., Chuvieco, E., Riano, D., Zylstra, P., Hunt Jr, E.R., Danson, F.M., Qi,  
621 Y. and Jurdao, S., 2013. A global review of remote sensing of live fuel moisture content for fire  
622 danger assessment: Moving towards operational products. *Remote Sensing of Environment*, 136,  
623 pp.455-468.
- 624 Zarco-Tejada, P.J., Rueda, C.A. and Ustin, S.L., 2003. Water content estimation in vegetation  
625 with MODIS reflectance data and model inversion methods. *Remote Sensing of Environment*,  
626 85(1), pp.109-124.



627 Zhao, T. and Dai, A., 2015. The magnitude and causes of global drought changes in the twenty-  
628 first century under a low–moderate emissions scenario. *Journal of climate*, 28(11), pp.4490-  
629 4512.

630

631

632

633

634

635

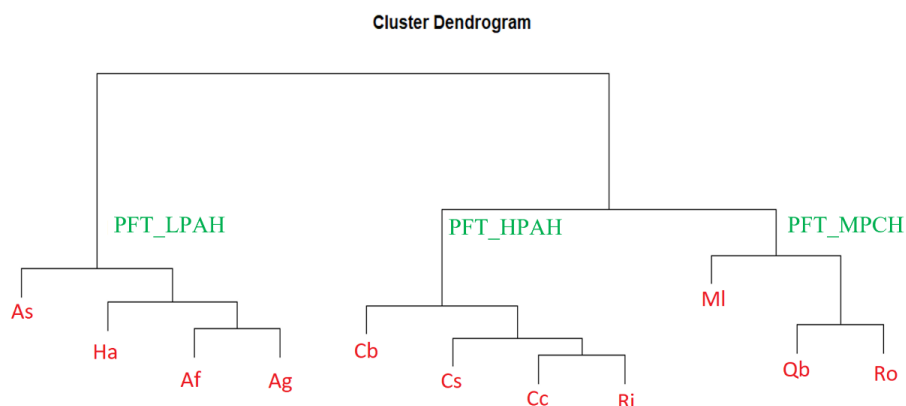
636

637

638

639

640



641

642 **Fig 1.** Hierarchical cluster analysis of allometry and hydraulic traits for eleven chaparral shrub  
643 species used to define three plant functional types at Stunt Ranch. The plant functional types  
644 with a Low Productivity and an Aggressive Hydraulic strategy (PFT\_LPAH) was defined based  
645 on traits of red shank (*Adenostoma sparsifolium* - As), toyon (*Heteromeles arbutifolia* - Ha),  
646 Chamise (*Adenostoma fasciculatum* - Af), big berry manzanita (*Arctostaphylos glauca* - Ag); the  
647 plant functional types with a High Productivity and an Aggressive Hydraulic strategy  
648 (PFT\_HPAH) was defined based on traits of mountain mahogany (*Cercocarpus betuloides* - Cb),  
649 greenbark ceanothus (*Ceanothus spinosus* - Cs), buck brush (*Ceanothus cuneatus* - Cc), hollyleaf  
650 redberry (*Rhamnus ilicifolia* - Ri); the plant functional types with a Medium Productivity and an  
651 Conservative Hydraulic strategy (PFT\_MPCH) was defined based on traits of laurel sumac  
652 (*Malosma laurina* - MI), scrub oak (*Quercus berberidifolia* - Qb), sugar bush (*Rhus ovata* - Ro).

653

654

655

656

657

658

659

660

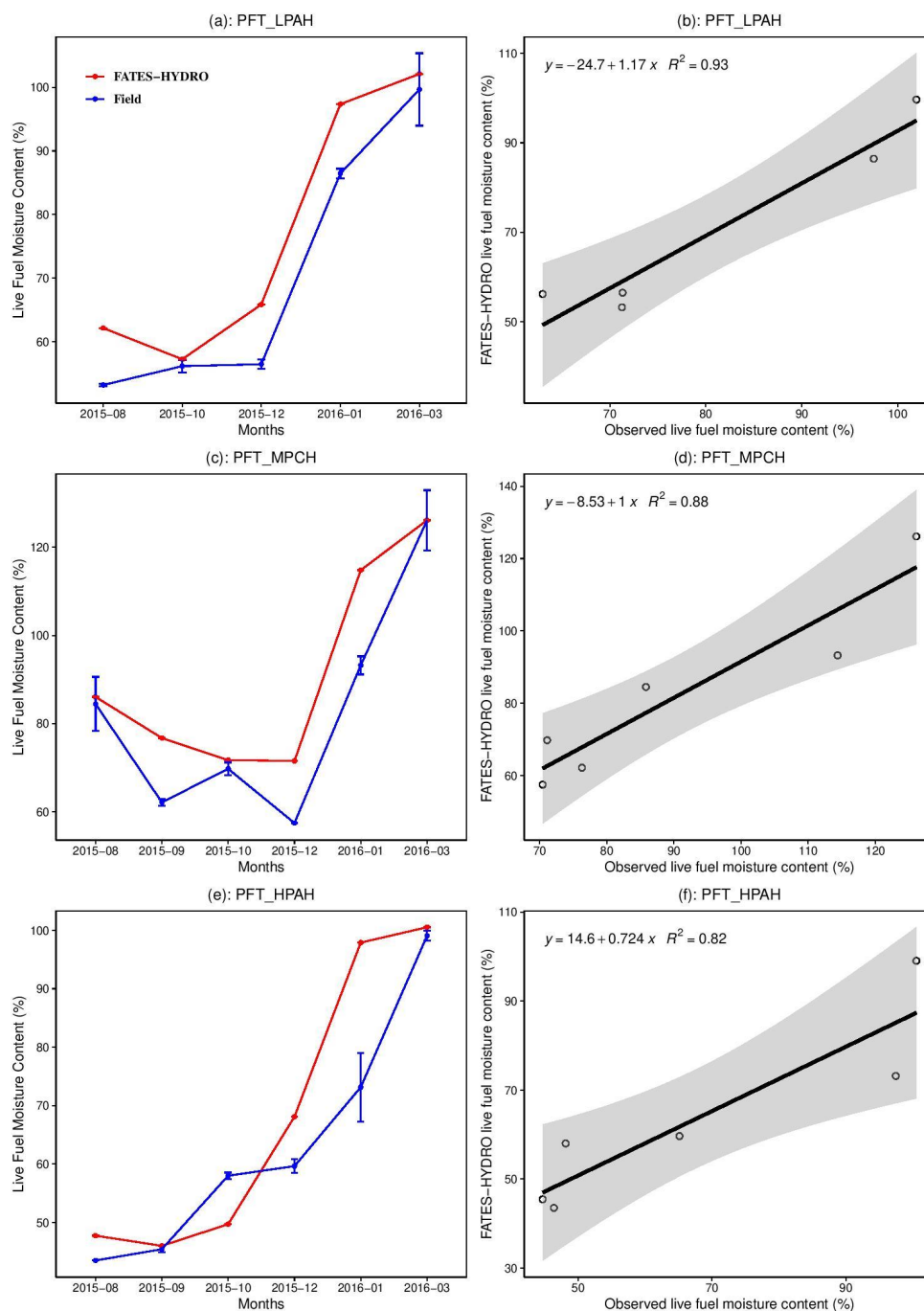
661

662

663

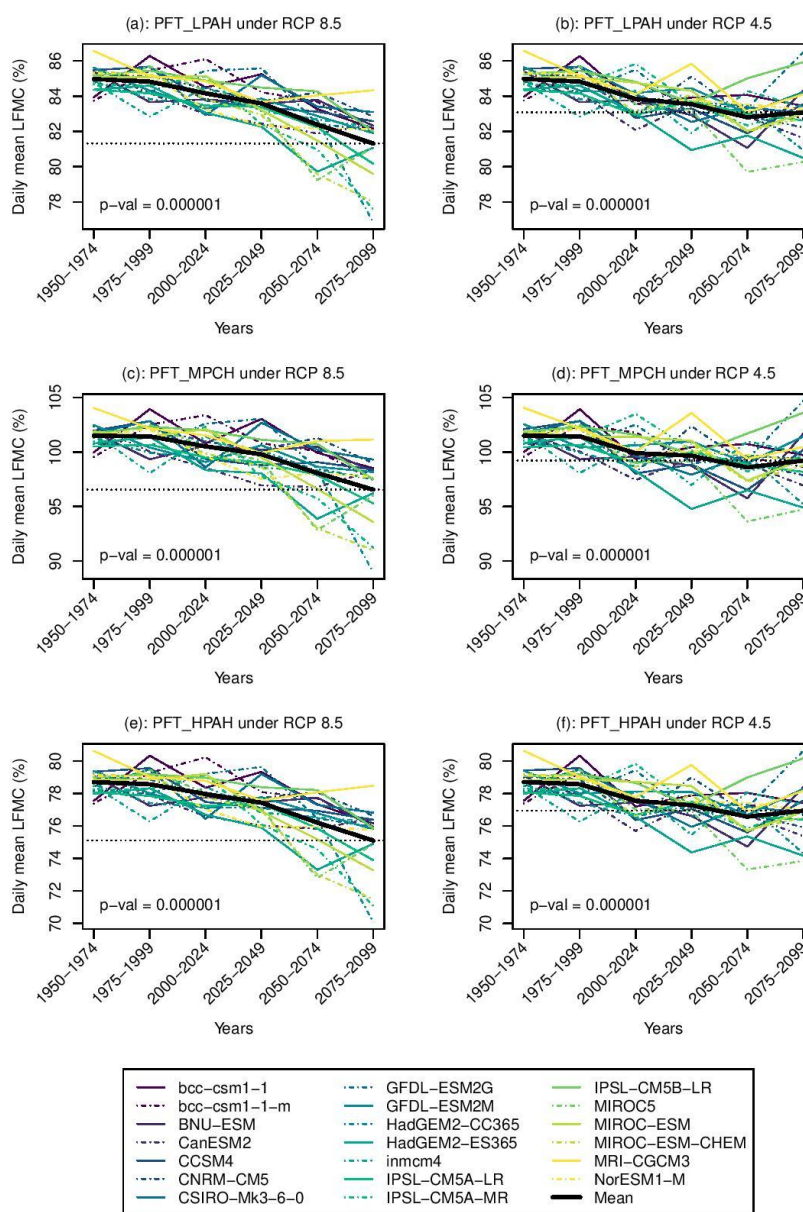
664

665



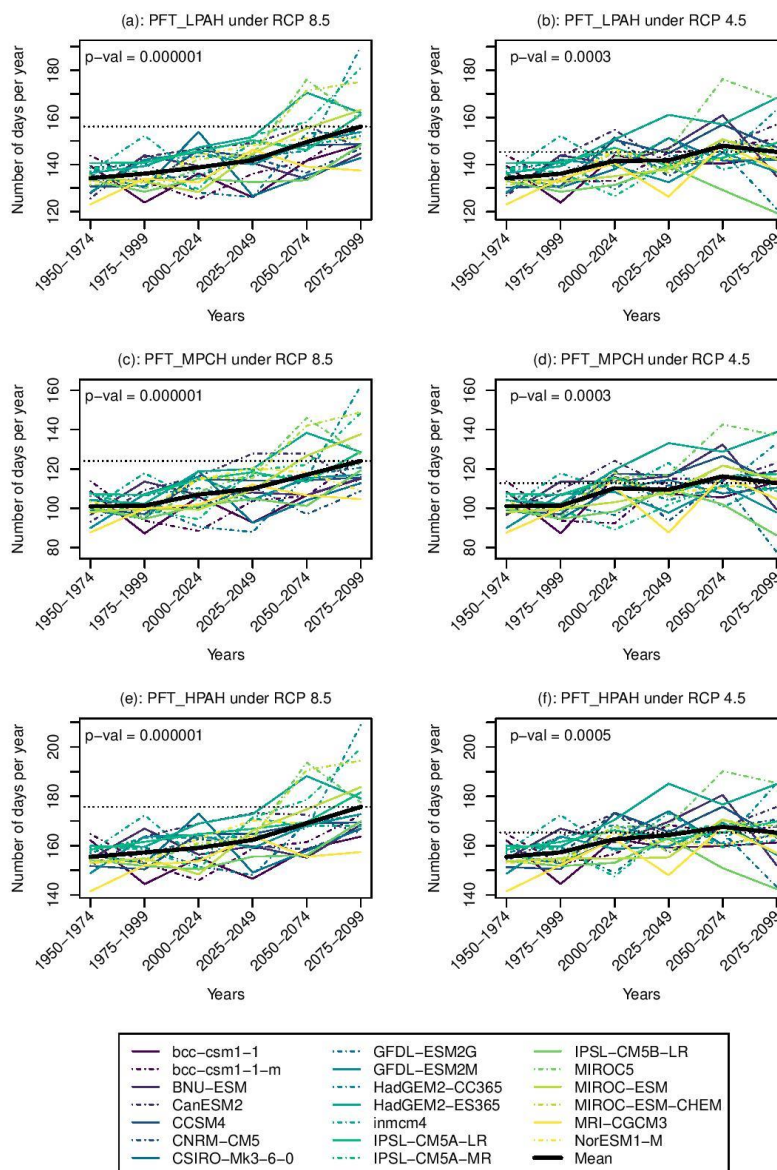
666

667 **Fig.2** Simulated and observed monthly live fuel moisture content and related  $R^2$  for three PFTs  
 668 (refer to Figure 1 for explanation of the PFTs).



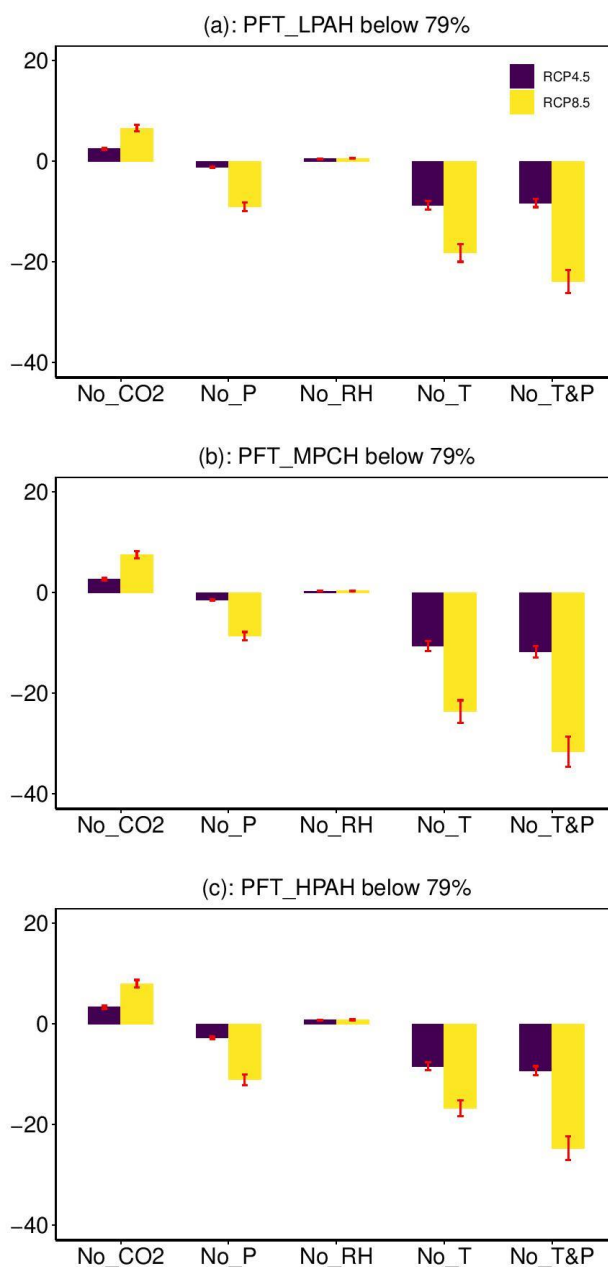
669

670 **Fig.3** Temporal changes in daily mean live fuel moisture content from 1950 to 2099 for three  
 671 PFTs (refer to Figure 1 for explanation of the PFTs) under climate scenario RCP 4.5 and 8.5  
 672 considering all climatic variables changes. The P values were calculated using bootstrap  
 673 sampling to test whether the daily mean live fuel moisture content across different models during  
 674 the future period (2075–2099) was significantly lower than that during the historical period  
 675 (1950–1999). The grey horizontal dotted line represents the ensemble mean for 2075–2099.



676

677 **Fig.4** Temporal changes in number of days per year of live fuel moisture content below 79%  
 678 from 1950 to 2099 for three PFTs (refer to Figure 1 for explanation of the PFTs) under climate  
 679 scenario RCP 4.5 and 8.5 considering all climatic variables changes. The P values were  
 680 calculated using bootstrap sampling to test whether the number of days across different models  
 681 during the future period (2075–2099) was significantly higher than that during the historical  
 682 period (1950–1999). The grey horizontal dotted line represents the ensemble mean for 2075–  
 683 2099.



684

685 **Fig.5** Differences on number of days per year of live fuel moisture content below 79% from  
686 2075 to 2099 for three PFTs (refer to Figure 1 for explanation of the PFTs) under climate  
687 scenario RCP 4.5 and 8.5 between considering all climatic variables changes and without  
688 considering CO<sub>2</sub>, precipitation, temperature, precipitation & temperature, relative humidity  
689 changes.